Angular effects in the energy loss of slow protons and helium ions transmitted through thin Al and Au films

C. D. Archubi, J. C. Eckardt, G. H. Lantschner, and N. R. Arista
División Colisiones Atómicas, Instituto Balseiro and Centro Atómico Bariloche, RA-8400 Bariloche, Argentina
(Received 14 November 2005; published 6 April 2006)

Measurements of the energy loss of 10 keV protons and helium ions in Al and Au as a function of the exit angle are presented, as well as model calculations and numerical simulations taking into account the polycrystalline nature of the target. The experimental results show significant differences in the angular dependence between hydrogen and helium ions. To analyze this phenomenon we have studied the angular behavior of the energy loss by two different approaches. The first one is based on a theoretical method described in previous works. The second is based on a simulation code which takes into account the interaction of the projectiles with all the nearest neighboring atoms simultaneously, and incorporates the real polycrystalline characteristics of the target as obtained by transmission electron microscopy. The results indicate that (a) the different angular behavior of helium ions is mainly due to an impact parameter dependence of the energy loss for these ions; and (b) additionally we find that the influence of the crystalline structure on the angular effects of the energy loss is small for protons and somewhat more significant for helium ions.

DOI: 10.1103/PhysRevA.73.042901 PACS number(s): 34.50.Bw, 78.20.Bh

I. INTRODUCTION

Energy loss and angular dispersion are two important parameters to characterize the penetration of energetic ions in matter and they have been extensively investigated for many years. Exhaustive measurements have been performed over the years to know the energy loss of ion beams traversing solid targets, but mostly in the ranges of intermediate and high energies. The energy loss is determined by several physical processes, such as the elastic collisions of the projectile with the cores of the atoms of the solid and the inelastic collisions with the electrons. Basic theoretical calculations of electronic energy loss of *slow* ions in solids (with velocities less than the mean velocity of valence electrons) using different approaches [1–4] predict a linear relationship between energy loss and ion velocity, as given by the expression

$$\frac{dE}{dx} = Qv, \tag{1}$$

where Q is a friction coefficient and v is the ion velocity. This coefficient has been calculated for transmitted particles in uniform media following different theoretical approaches (linear and nonlinear models) based on free-electron approximations. In the last two decades nonlinear effects have been studied using density functional theory to describe ion-electron interactions [3–5].

On the other hand, additional topological factors (such as foil roughness and density inhomogeneities) have been proved to be relevant for the determination of the behavior of the energy loss as a function of the exit angle after traversing thin solid foils. These angular effects in the energy loss of light ions have been studied during more than two decades in the ranges of medium [6–9], high [10], and low energies [11], showing important differences appearing at low energies. Some of these differences are a direct consequence of the larger dispersion angles occurring at lower energies, such as, for instance, the geometric path length enlargement or the increasing importance of the elastic energy loss at nonzero observation angles. In addition, it may be expected that the effects of target texture could play an important role. Hence it becomes relevant to clarify the relative importance of these various effects and to determine to what extent these effects may have some influence on experimental determinations of stopping coefficients of slow ions.

A previous model [11], which explains in a satisfactory way the angular dependence observed for protons in various targets, is based on a phenomenological description of three main contributions: elastic energy losses, path-length enlargement (inelastic energy loss increase), and foil-roughness effects.

More recently, we have applied a simulation scheme to the angular dispersion of ions in solids [12,13] based on deterministic trajectory calculations, taking into account the crystalline structure, and including the effects of the polycrystalline characteristics observed in the foils [studied with transmission electron microscopy (TEM)], including grain size and the presence of twins, as well as thermal lattice vibrations and foil roughness effects.

In this work we compare the results obtained from the theoretical model and the results of the simulations with the experimental ones for the cases of hydrogen and helium beams, with incident energies of 10 keV, traversing thin foils of gold and aluminum. In previous experiments [14] we have shown that currently used theoretical models for metals are not always adequate for quantitative evaluations of the friction coefficients for hydrogen and helium ions in the low energy range. The present work extends the previous analysis to the angular dependence of the energy loss and therefore provides more complete information on this phenomenon.

In the next section we describe the experimental method and the theoretical approaches used in this work. In Sec. III we show the experimental results for the angular dependence of the energy loss of hydrogen and helium ions after passing

through Al and Au foils, including comparisons with the results of the theoretical model and the numerical simulations. In this section we also analyze the influence of crystalline target structure on angular behavior of the energy loss. Finally, Sec. IV contains a summary and the final conclusions of this work.

II. EXPERIMENTAL AND THEORETICAL APPROACHES

A. Experimental method

The energy loss determinations presented here were made by the transmission method with an experimental arrangement described previously [11,12]. The H^+ and He^+ beams were generated by electrostatic acceleration of ions produced in a hot discharge ion-source. Electrostatic focusing, Wien-filter mass selection stages, and collimation defined the final beam. The energy-angle analysis was performed by a rotatable electrostatic analyzer with 1% energy resolution yielding an angular resolution of 1.9°. The particles were detected by a discrete dynode electron multiplier followed by conventional pulse counting electronics. Spectra were recorded by a multichannel scaler with channels switched synchronously with the energy analyzer plate potential. Self-supported polycrystalline targets were made by evaporation under clean vacuum conditions on a very smooth plastic substrate [15] which was subsequently dissolved. The foil thickness of the polycrystalline target was determined by matching proton energy-loss measurements to the stopping power values of Valdés *et al.* [16] yielding 13.1 nm in the case of gold and 18.8 nm in the case of aluminum. The smoothness of the foils was checked by the method described in Ref. [17]. The result was an estimated upper bound to the roughness ρ of 14% in both cases (gold and aluminum films), with ρ defined as the variance of the foil thickness distribution relative to the mean foil thickness. The crystalline structure was analyzed by transmission electron microscopy.

Foil thickening by ion beam bombardment was held within negligible limits by using a low ion current density of $\sim 10^{-11}$ A/mm^2, and irradiation times of less than 2 min per spectrum. In this way no change in foil characteristics could be detected during the time of measurements.

B. Theoretical model

In a previous publication [11] an analytical model was proposed to explain the angular behavior of the energy loss of protons and deuterons passing through thin aluminum and gold films, considering the three following contributions: (a) path enlargement and subsequent increase of the electronic stopping, (b) foil roughness effect, and (c) elastic energy loss. The electronic energy loss is calculated in this model assuming a constant friction coefficient Q, and an amorphous target structure.

The result of this model is summarized by the following expression:

$$\Delta E(\theta) - \Delta E(0) = \Delta E_{path}(\theta) + \Delta E_{rough}(\theta) + \Delta E_{elastic}(\theta), \tag{2}$$

where θ is the angle of emergence of the projectile after passing through the foil, $\Delta E(0)$ is the energy loss measured at zero angle of emergence (forward direction), $\Delta E_{path}(\theta)$ the effect of path enlargement on the electronic energy loss, $\Delta E_{elastic}(\theta)$ is the contribution of the nuclear elastic stopping, and $\Delta E_{rough}(\theta)$ is the contribution of the foil roughness.

The elastic energy loss is given by

$$\Delta E_{elastic}(\theta) \simeq \frac{4M_1M_2}{(M_1+M_2)^2} E \sin^2(\theta/2), \tag{3}$$

where M_1 and M_2 are the respective projectile and target masses, E is the mean energy of the projectiles, and θ the corresponding exit angle. The analytical expressions for $\Delta E_{path}(\theta)$ and $\Delta E_{rough}(\theta)$ are given in Ref. [11].

C. Simulation method

The main lines of our simulation method have been detailed in previous works [12,13]. In the simulations the crystal structure is taken into account situating the ion within the central cell of a cluster of $3\times3\times3$ fcc cells. The resultant force of the interaction of the ion with all the surrounding atoms inside this cluster, up to a distance equivalent to one lattice constant, is derived for different types of screened Coulomb potentials. As we have shown in previous works [12,13], a good description of the angular distribution may be obtained using a modified Molière potential. The trajectory of the ion is obtained by the discretization of the standard kinematic equations into small time steps. Each time the ion exits the central cell of the cluster a new slab of 3×3 cells is generated in the corresponding direction and the backward slab of cells is eliminated. Therefore the projectile is always in the central cell of a $3\times3\times3$ cluster.

The different starting points of the projectile when it hits the foil are simulated randomizing the initial position inside the central cell of the first cluster. In the case of a polycrystal the different random orientations of the microcrystals are simulated by randomizing the initial direction of the projectile relative to the principal axes of the crystal. When the ion crosses the boundary between two microcrystals within the foil the direction of the new microcrystal is again simulated by randomly changing its orientation. Finally, since the experiments are performed at room temperature, our simulations also contemplate the effect of thermal vibrations. A typical simulation involves between 5×10^5 and 10^6 ion trajectories.

The angular dependences of the energy loss are obtained recording the final energy and emergence angle of each ion after a number of time steps corresponding to the target thickness x and considering an electronic energy loss dE for each path-step dx given by

$$dE = Q(r)v\,dx, \tag{4}$$

where $Q(r)$ is the low-velocity friction coefficient of the projectile at a distance r from the nearest target atom and v is the instantaneous velocity of the projectile.

The value of the friction coefficient is represented here using two alternative approaches: (i) we assume a constant value of this coefficient, Q=constant, which corresponds to the experimental value of the energy loss in the beam direc-

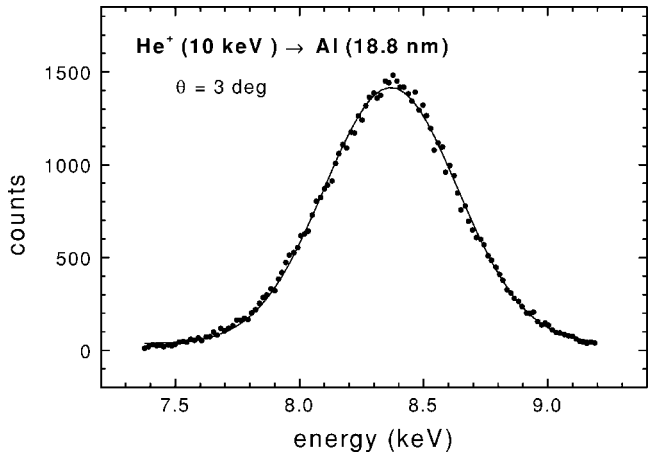

FIG. 1. Energy spectrum of 10 keV He^+ ions after traversing an aluminum foil of 18.8 nm thickness. The solid line is a Gaussian fit.

tion, namely $Q=\Delta E(0)/\langle v\rangle x$ where the mean velocity $\langle v\rangle$ is obtained from the experimental value of the medium energy $\langle E\rangle$ of the projectile inside the foil [16,18], or (ii) we propose an analytical expression of the form $Q(r)=Ae^{-\alpha r}$ where A and α are fitting constants and r is the distance of the projectile to the nearest target atom.

With the corresponding value of the instantaneous energy loss we calculate the modification of the velocity components of the projectile for each step of the trajectory.

We also include in the simulations the effect of foil roughness. To do this, we consider different thicknesses for each ion in the simulation, following a Gaussian distribution with a standard deviation corresponding to the experimental foil roughness.

III. RESULTS AND INTERPRETATIONS

In Fig. 1 we show a typical energy spectrum, in this case corresponding to 10 keV He^+ ions after traversing a 18.8 nm Al foil. One can observe the Gaussian shape which allows an unambiguous and precise determination of the mean energy.

The experimental energy loss results are shown in Figs. 2 and 3, together with the theoretical model calculations, where we show the differences $\Delta E(\theta)-\Delta E(0)$ for protons and helium ions traversing the same foil. In Fig. 2 we can appreciate the total result for the angular behavior of the energy loss calculated with the theoretical model and compared with the experimental results for the case of protons and helium ions traversing a 13.1 nm thick Au foil. In Fig. 3 we show similar results for protons and helium ions traversing a 18.8 nm thick Al foil. One can observe in these figures important differences for both ions.

Two methods have been used in order to interpret the experimental results. The first one is based on the theoretical model mentioned in the previous section. The second one is based on a simulation code which permits us to evaluate the influence of the crystalline structure as well as the influence of the r--dependence in the friction coefficient associated to the electronic energy loss.

The results of the first method are shown in Figs. 2 and 3 and compared with the experimental results for hydrogen

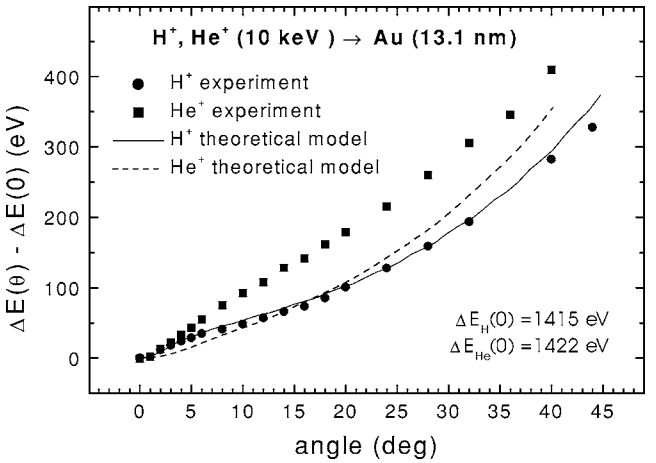

FIG. 2. Comparison between the experimental results and the results obtained from the theoretical model. The solid circles and squares represent the experimental results for the energy loss of 10 keV protons and helium ions passing through a 13.1 nm gold polycrystal. The full line and the dashed line are the result obtained with the model for protons and helium ions. The value of the roughness considered here is 11%.

and helium ions in gold and aluminum. As shown by these figures, the comparison between theoretical models and experiments is fairly good for hydrogen while a significant disagreement is observed for helium. We found that these discrepancies could not be explained with the proposed theoretical model and hence we have studied them using the simulation code described before.

The results of the simulations are shown in Figs. 4 and 5, and they are compared with the experimental results for hydrogen and helium ions traversing the Au and Al foils indicated before. In the case of protons, the difference between the experimental results and the simulations assuming ap-

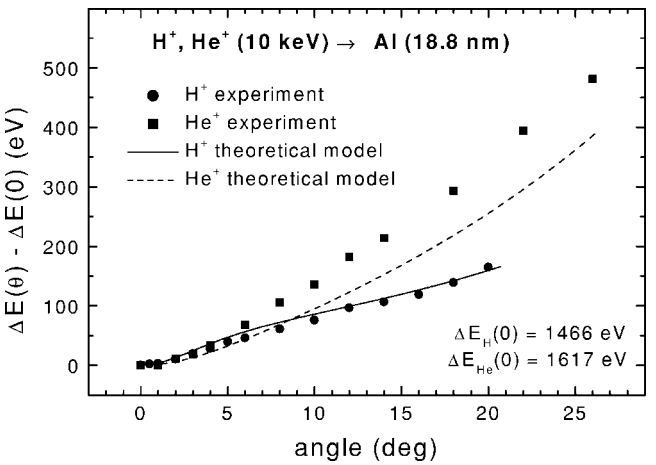

FIG. 3. Comparison between the experimental data and the results obtained from the theoretical model. The solid circles and squares represent the experimental results for the energy loss of 10 keV protons and helium ions passing through a 18.8 nm aluminum polycrystal. The full and dashed lines are the results obtained with the model. The value of the roughness considered for this fitting is 14%.

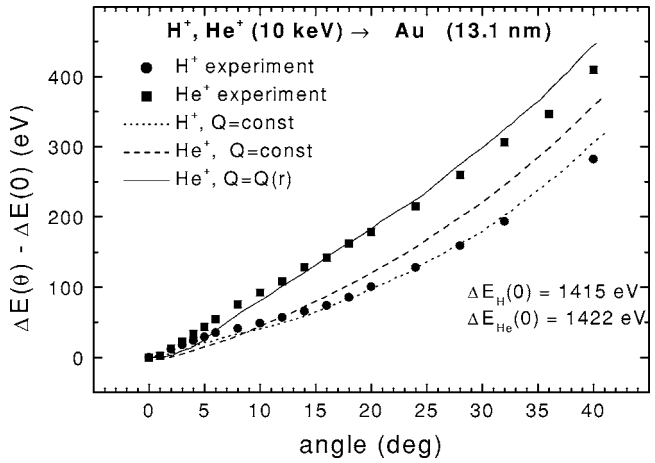

FIG. 4. Comparison between the experimental results and the results obtained from the numerical simulations for 10 keV protons (dotted line) and helium ions (dashed and full lines) passing through a 13.1 nm gold polycrystal considering two different procedures: (i) Q=const (dashed line), and (ii) $Q=Q(r)$ (full line). To include an r-dependent $Q(r)$ we have used the fitting expression $Q(r)=C_1\exp(-0.3r)$ where C_1 is a constant adjusted in order to obtain the experimental value for the energy loss $\Delta E(0)$. The simulations include a foil roughness of 11%.

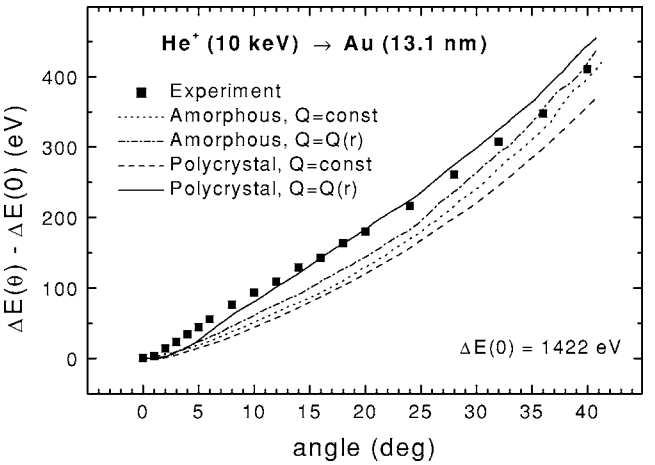

FIG. 6. Comparison between simulation results for 10 keV helium ions passing through a 13.1 nm gold target. The simulation includes a foil roughness of 11%. It can be observed that there is a difference between the simulation results assuming an amorphous target with Q=const (dotted line) and with $Q=Q(r)$ (dash-dot line), but this is smaller than the corresponding difference between the results with Q=const (dashed line) and $Q=Q(r)$ (full line) obtained for a polycrystal.

proach (i) (constant stopping coefficient) are found to be very small, so that it was not necessary to use the second approach. However, in the case of helium ions we do observe important differences between the experiments and the simulations using the constant-Q assumption. In this case the use of an inhomogeneous friction coefficient $Q(r)$ as indicated in (ii) yields a remarkable improvement, as it is clearly illustrated in Figs. 4 and 5.

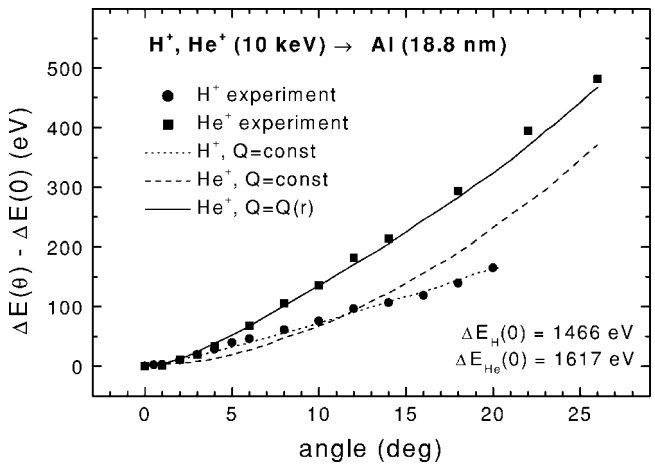

FIG. 5. Comparison between the experimental results and the results obtained from the numerical simulations for 10 keV protons (dotted line) and helium ions (dashed and full lines) passing through a 18.8 nm aluminum polycrystal considering two different procedures: (i) Q=const (dashed line), and (ii) $Q=Q(r)$ (full line). To include an r-dependent $Q(r)$ we have used the fitting expression $Q(r)=C_2\exp(-0.6r)$ where C_2 is a constant adjusted in order to obtain the experimental value for the energy loss $\Delta E(0)$. The simulations include a foil roughness of 14%.

The values $\Delta E(0)$ inserted in Figs. 2–7 are the experimental values of the energy loss at zero angle (*forward energy loss*). As in previous works [14,16] we may compare these values with those predicted by the density functional theory (DFT) [4], which considers a slow ion moving through a uniform electron gas with an average density n_e represented by the parameter r_s (with $4\pi r_s^3/3=1/n_e$). Taking into account only the free electrons in aluminum (r_s=2.07 a.u.) and an effective number of *quasifree* electrons in Au ($r_s\cong 1.5$ a.u.), and considering the experimental thickness values (188 Å

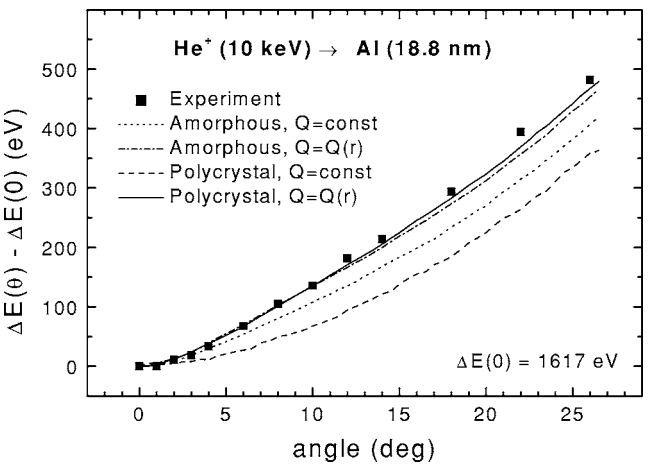

FIG. 7. Comparison between simulation results for 10 keV helium ions passing through an 18.8 nm aluminum target. The simulations include a foil roughness of 14%. It can be observed that there is a difference between the simulation results assuming an amorphous target with Q=const (dotted line) and $Q=Q(r)$ (dash-dot line), but this is smaller than the corresponding difference between the results with Q=const (dashed line) and $Q=Q(r)$ (full line) obtained for a polycrystal.

for Al and 131 Å for Au) we obtain the expected energy losses of H and He, after a spline interpolation of the values tabulated by Puska and Nieminen [4]. In this way we obtain:

$$\Delta E_{DFT}[\mathrm{H} \rightarrow \mathrm{Al}] = 1.54 \text{ keV}, \quad (5)$$

$$\Delta E_{DFT}[\mathrm{He} \rightarrow \mathrm{Al}] = 1.15 \text{ keV}, \quad (6)$$

$$\Delta E_{DFT}[\mathrm{H} \rightarrow \mathrm{Au}] = 1.27 \text{ keV}, \quad (7)$$

$$\Delta E_{DFT}[\mathrm{He} \rightarrow \mathrm{Au}] = 1.55 \text{ keV}, \quad (8)$$

which may be compared with the experimental values: 1.466, 1.617, 1.415, and 1.422 keV, respectively. The differences between the theoretical predictions and the experimental results are of 5%–10%, except for the case of He ions in Al, where the DFT value falls ~30% below the experiment. We may note that this level of agreement is similar to the one previously reported in Ref. [14], including the larger discrepancy for He in Al; so that the present experiments fully confirm the previous determinations of forward energy losses.

In summary, the angular dependence of the energy loss of hydrogen ions appears to be very well represented by the analytical model as well as by the numerical simulations assuming a nearly constant (within the limits of the experimental resolution and of the fluctuations of the current simulations) friction coefficient Q. These results are in agreement with those obtained by Famá *et al.* [11] for protons in the same energy range. By contrast, the results for helium ions show a distinct angular dependence that can only be explained via the introduction of an r-dependent friction coefficient in the simulations (note that this is equivalent to consider an impact parameter dependence of the energy transfer, as is usually done at higher energies [19], and is also similar to previous descriptions considering an inhomogeneous electron gas description at low energies [20]).

Influence of the crystalline structure

To evaluate the influence of the crystalline structure we have applied the simulation method described before. To make a realistic representation of the targets they were analyzed by TEM. The gold target was composed of randomly oriented microcrystals of irregular shapes and different sizes in the range of 5–40 nm. We estimate that approximately 60% of the foil was composed of a single layer of these microcrystals and the other 40% was composed by two overlapped layers of microcrystals. The simulations were performed considering these percentages.

In the case of aluminum, the target was composed by randomly oriented microcrystals of irregular shapes but more regular sizes in the range of 20 nm. Thus we have considered it composed of a single layer of microcrystals. We have also considered in the case of aluminum, the presence of oxide. Based on specific studies [21], we assume that the thickness of the oxide layer is 2 nm, at each side of the foil. To simulate this oxide layer we consider an amorphous region of cells (three atoms of oxygen and two atoms of aluminum per cell) at each side of the foil.

As can be observed by comparing the solid lines in Figs. 2 and 3, and the dotted lines in Figs. 4 and 5 in the case of protons both methods (the theoretical model considering an amorphous structure, and the simulations considering a polycrystalline structure) reproduce fairly well the experimental results.

In Figs. 6 and 7 we show the results of our simulations for helium ions considering amorphous and polycrystalline target structures and the two previously mentioned assumptions for the friction coefficient Q, namely: (i) Q=constant, and (ii) $Q=A\exp(-\alpha r)$.

However, the assumption of a variable Q is not enough to explain the results in the case of helium ions in gold if we keep the assumption of an amorphous structure, as it is shown in Fig. 6. It is when both effects are considered (crystalline structure and r-dependence of Q) that we can reproduce fairly well the experimental results.

Finally we note that, in contrast with the large influence of the crystalline structure on the behavior of the *angular distribution* of protons studied in previous works [12,22], the influence of these crystalline characteristics on the angular behavior of the *energy loss* is comparatively very small, being somewhat more important in the case of helium ions.

IV. SUMMARY AND CONCLUSIONS

We have performed comparative transmission measurements of the angular behavior of the energy losses of 10 keV protons and helium ions in polycrystalline foils of gold and aluminum. The polycrystalline structure of these foils has been determined using TEM techniques. Interesting differences in the angular behavior of the energy loss of protons and helium ions in both foils have been observed. To interpret these differences we have studied the subject using two methods. The first method is a theoretical model and the second one is based on a simulation code.

The theoretical model is based on two assumptions: (a) the foil is represented as an amorphous medium, and (b) the electronic energy loss of slow ions may be represented by Eq. (1) using a mean value of the friction coefficient Q. These assumptions appear to hold as good approximations in the case of hydrogen, where the influence of the crystalline structure in the angular dependence of the energy loss, studied in detail with the simulation method, was found to be very small.

In the case of helium ions there are important discrepancies between the theoretical model and the experimental results. We find that the computational results improve when we consider an r-dependent friction coefficient Q, taking into account the local dependence of the electronic energy loss. Moreover, the results of our simulation show that the influence of the crystalline structure is not negligible because the consideration of a local dependence of the energy loss is not enough to eliminate the above-mentioned discrepancies, and the agreement with the experiments improves significantly when we take into account the crystalline nature of the target.

The different behavior of hydrogen and helium appears to be a very interesting feature for the theoretical analysis, although a simple explanation cannot be given here. From a physical point of view we may note that at these energies

both hydrogen and helium projectiles should be mostly neutral, helium being a much smaller system than hydrogen (and so it senses in a more local way the electronic properties of the medium). A theoretical treatment of the angular dependence of the energy loss should take not only this into account, but also the effects of the inhomogeneities in the electron densities of the material, modified by the presence of a moving intruder atom, as well as a full treatment of the nonlinear effects. The density functional calculations of friction coefficients available so far [3,4] consider a homogeneous medium and a nearly static ion, neglecting also other dynamic phenomena such as charge exchange. As we have previously shown [14], these models cannot reproduce quantitatively the experimental stopping power values for protons and helium ions in various metals at low energies. In this respect, the present experimental results extend the previous ones to the angular dependence of the energy loss and therefore provide a still more stringent test for future theoretical evaluations.

In conclusion, it seems that further investigations of the angular dependence of the energy loss of hydrogen and helium ions in the low-energy range, using well-characterized foils of various materials, could provide important information on the phenomenon of angular dispersion and crystalline effects in the energy loss, yielding also information of intrinsic interest for improved theoretical descriptions of the energy loss phenomenon.

ACKNOWLEDGMENTS

This work was partially supported by the Argentine ANPCYT (Grant No. PICT-R00122/02) and CONICET (Grant No. PIP 02841). C.D.A. wishes to thank the CONICET for support.

[1] J. Lindhard, K. Dan. Vidensk. Selsk. Mat. Fys. Medd. **28**, 1 (1954).
[2] T. L. Ferrell and R. H. Ritchie, Phys. Rev. B **16**, 115 (1977).
[3] P. M. Echenique, R. M. Nieminen, and R. H. Ritchie, Solid State Commun. **37**, 779 (1981); I. Nagy, A. Arnau, and P. M. Echenique, Phys. Rev. A **40**, 987 (1989).
[4] M. J. Puska and R. M. Nieminen, Phys. Rev. B **27**, 6121 (1983).
[5] *Interaction of Charged Particles with Solid and Surfaces*, Vol. 271 of *NATO Advanced Study Institute, Series B: Physics*, edited by A. Gras-Marti, H. M. Urbassek, N. R. Arista, and F. Flores (Plenum, New York, 1991).
[6] G. A. Iferov and Yu. N. Zhukova, Phys. Status Solidi B **110**, 653 (1982); G. A. Iferov, V. A. Khodyrev, E. I. Sirotinin, and Yu. N. Zhukova, Phys. Lett. **97A**, 283 (1983); L. Meyer, Phys. Status Solidi B **44**, 253 (1971).
[7] A. A. Bednyakov, V. Ya. Chumanov, O. V. Chumanova, G. A. Iferov, V. S. Kulikauskas, I. I. Rasgulyaev, and Yu. N. Zhukova, Nucl. Instrum. Methods Phys. Res. B **115**, 168 (1996).
[8] J. C. Eckardt, G. H. Lantschner, M. M. Jakas, and V. H. Ponce, Nucl. Instrum. Methods Phys. Res. B **2**, 168 (1984).
[9] M. Famá, J. C. Eckardt, G. H. Lantschner, and N. R. Arista, Phys. Rev. Lett. **85**, 4486 (2000).
[10] R. Iishiwari, N. Shiomi, N. Sakamoto, and H. Ogawa, Nucl. Instrum. Methods Phys. Res. B **13**, 111 (1986); R. Iishiwari, N. Shiomi-Tsuda, N. Sakamoto, and H. Ogawa, *ibid.* **51**, 209 (1990).
[11] M. Famá, G. H. Lantschner, J. C. Eckardt, C. D. Denton, and N. R. Arista, Nucl. Instrum. Methods Phys. Res. B **164–165**, 241 (2000).
[12] C. Archubi, C. D. Denton, J. C. Eckardt, G. H. Lantschner, F. Lovey, J. Valdés, C. Parra, F. Zappa, and N. R. Arista, Phys. Status Solidi B **241**, 2389 (2004).
[13] C. Archubi, C. D. Denton, J. C. Eckardt, G. H. Lantschner, J. Valdés, J. Ferrón, and N. R. Arista, Nucl. Instrum. Methods Phys. Res. B **230**, 53 (2005).
[14] G. Martínez-Tamayo, J. C. Eckardt, G. H. Lantschner, and N. R. Arista, Phys. Rev. A **54**, 3131 (1996).
[15] A. Valenzuela and J. C. Eckardt, Rev. Sci. Instrum. **42**, 127 (1971).
[16] J. E. Valdés, G. Martínez-Tamayo, G. H. Lantschner, J. C. Eckardt, and N. R. Arista, Nucl. Instrum. Methods Phys. Res. B **73**, 313 (1993).
[17] J. C. Eckardt and G. H. Lantschner, Thin Solid Films **249**, 11 (1994).
[18] R. Blume, W. Eckstein, and H. Verbeek, Nucl. Instrum. Methods **168**, 57 (1980).
[19] P. L. Grande and G. Schiwietz, Phys. Rev. A **58**, 3796 (1998); G. Schiwietz and P. L. Grande, Nucl. Instrum. Methods Phys. Res. B **153**, 1 (1999); G. M. de Azevedo, P. L. Grande, and G. Schiwietz, *ibid.* **164**, 203 (2000).
[20] P. Vargas, J. E. Valdés, and N. R. Arista, Phys. Rev. A **53**, 1638 (1996).
[21] N. Cabrera and N. F. Mott, Rep. Prog. Phys. **12**, 163 (1949).
[22] H. H. Andersen, J. Bottiger, H. Knudsen, and P. Moller-Petersen, Phys. Rev. A **10**, 1568 (1974).